AFRL-VS-HA-TR-2004-1193
E.R.P., No. 1259

Cloud Optical Depth Retrieval from Cloud Radar and Microwave Radiometer Measurements

Paul R. Desrochers

5 Nov 2004

Approved for Public Release; Distribution Unlimited

AIR FORCE RESEARCH LABORATORY
Space Vehicles Directorate
29 Randolph Rd
AIR FORCE MATERIEL COMMAND
Hanscom AFB, MA 01731-3010

AFRL-VS-HA-TR-2004-1193

This technical report has been reviewed and is approved for publication.

Robert A. Morris, Chief
Battlespace Environment Division

Paul R. Desrochers
Author

Robert Beland, Chief
Battlespace Surveillance Innovation Center

This report has been reviewed by the ESC Public Affairs Office (PA) and is releasable to the National Technical Information Service (NTIS).

Using Government drawings, specifications, or other data included in this document for any purpose other than Government procurement does not in any way obligate the U.S. Government. The fact that the Government formulated or supplied the drawings, specifications, or other data does not license the holder or any other person or corporation; or convey any rights or permission to manufacture, use, or sell any patented invention that may relate to them.

This report is published in the interest of scientific and technical information exchange and its publication does not constitute the Government's approval or disapproval of its ideas or findings.

Qualified requestors may obtain additional copies form the Defense Technical Information Center (DTIC). All others should apply to the National Technical Information Service.

If your address has changed, if you wish to be removed from the mailing list, or if the addressee is no longer employed by your organization, please notify AFRL/VSIM, 29 Randolph Rd., Hanscom AFB, MA 01731-3010. This will assist us in maintaining a current mailing list.

Do not return copies of this report unless contractual obligations or notices on a specific document require that it be returned.

REPORT DOCUMENTATION PAGE

Form Approved
OMB No. 0704-0188

PLEASE DO NOT RETURN YOUR FORM TO THE ABOVE ADDRESS.

1. REPORT DATE *(DD-MM-YYYY)*	2. REPORT TYPE	3. DATES COVERED *(From - To)*
05-11-2004	Scientific, Interim	

4. TITLE AND SUBTITLE
Cloud Optical Depth Retrieval from Cloud Radar and Microwave Radiometer Measurements

5a. CONTRACT NUMBER

5b. GRANT NUMBER

5c. PROGRAM ELEMENT NUMBER
62601F

6. AUTHOR(S)
Paul R. Desrochers

5d. PROJECT NUMBER
1010

5e. TASK NUMBER
BS

5f. WORK UNIT NUMBER
A1

7. PERFORMING ORGANIZATION NAME(S) AND ADDRESS(ES)
Air Force Research Laboratory/VSBYM
29 Randolph Road
Hanscom AFB. MA 01731-3010

8. PERFORMING ORGANIZATION REPORT NUMBER
AFRL-VS-HA-TR-2004-1193
Environmental Research Papers, No. 1259

9. SPONSORING/MONITORING AGENCY NAME(S) AND ADDRESS(ES)

10. SPONSOR/MONITOR'S ACRONYM(S)

11. SPONSOR/MONITOR'S REPORT NUMBER(S)

12. DISTRIBUTION/AVAILABILITY STATEMENT
Approved for public release; distribution unlimited.

13. SUPPLEMENTARY NOTES

14. ABSTRACT
Radar and microwave radiometer measuremens of clouds were taken along the California coast at Vandenberg AFB on 10 Sept. and 18 Oct. 2003 in conjunction with Minuteman III and Titan II rocket launches. The purpose was to characterize the clouds to derive an estimate of the optical depth at the time of the launches. These measurements support the Signature Exploitation Program development effort at AFRL to detect rocket emissions through optically thick clouds. The instruments used were the Air Force Research Laboratory Ka-band (35 GHz) Doppler radar, termed the Air Force Cloud Profiling Radar and a Radiometrics Corp. model WVQ-1500, 5-channel (22-30 GHz) water vapor profiling microwave radiometer. A variation of the technique developed by Frisch et al. used radar backscatter and microwave radiometer derived total integrated liquid water to yield an estimate of the cloud droplet number density and the vertical profile of the droplet effective radius. The cloud droplet distribution is approximated by a lognormal distribution. Climatology is used to select the distribution width. The retrieved cloud characteristics are applied to the Wiscombe Mie scattering codes augmented for optical depth calculations. An optical depth of 68 was obtained near the time of the 10 Sept. launch. No useful retrieval resulted from the 18 Oct. case because the skies were clear overhead.

15. SUBJECT TERMS
Optical depth
Radar
Microwave radiometer
Fog

16. SECURITY CLASSIFICATION OF:			17. LIMITATION OF ABSTRACT	18. NUMBER OF PAGES	19a. NAME OF RESPONSIBLE PERSON
a. REPORT	b. ABSTRACT	c. THIS PAGE			Paul R. Desrochers
UNCL	UNCL	UNCL	UNL		19b. TELEPHONE NUMBER *(Include area code)* (781) 377-2948

Contents

Illustrations

Tables

Acknowledgments

The author wishes to thank MSgt James Abshire, whose tireless efforts ensured that the radar was operational for these Vandenberg tests. I am also grateful to Daniel DeBenedictis of Titan Corp. for providing the MM5 model run.

1. INTRODUCTION

The optical depth of a cloud is a function of the path length through the cloud, the drop size distribution and the number density. If these parameters are known, the optical depth can be calculated through application of Mie scattering theory. The objective of the present investigation is to determine the cloud optical depth near the time of several rocket launches at Vandenberg AFB, located along the California coast.

Cloud optical depth has been shown to be directly related to the total liquid water content (LWC) (e.g., Stevens, 1978). Therefore, the accuracy of the retrieval will be largely governed by the accuracy in retrieved liquid content. Among the most accurate methods of retrieving the integrated cloud liquid water content is through the use of a multi-channel ground based microwave radiometer (MWR) (e.g., Hogg et al., 1983). MWRs have undergone extensive refinement and testing in support of the Atmospheric Radiation Measurement (ARM) program (Revercomb, 2003). The thermal accuracy for modern, self-calibrating systems is generally within 0.5° C (Solheim et al., 1996; Solheim et al.; 1998; Westwater et al., 2000; Cimini et al., 2003).

In addition to the integrated liquid water content, optical depth is governed by the distribution of drop sizes. The goal of the present investigation is to determine the cloud optical depth (τ) at Visible and Near Infrared Wavelength (NIR). At NIR τ will be more sensitive to cloud droplets, which generally have a modal radius of ~10 microns or less, and less sensitive to the larger size rain drops. Modern Ka-band and W-band "cloud radars" have adequate sensitivity to detect non-precipitating clouds.

Frisch et al. (1995, 1998) describe a cloud radar/microwave radiometer technique that provides estimates of the cloud droplet microphysical characteristics. The technique uses range gate averaged radar reflectivity together with MWR-derived total integrated water to provide the height profile of cloud droplet effective radius (r_e) and cloud liquid water. Frisch et al. (2002) report that the radar/radiometer-derived effective radius estimates agree within 19% to aircraft in situ effective radius measurements using a forward scattering spectrometer probe (FSSP). Likewise, liquid water estimates are also found to agree to in situ aircraft measurements, within 0.02 g/m^3 according to Frisch et al. (2000).

Marine stratus clouds, which are a common feature to the California coast, are likely to contain an active drizzle process. One consideration in applying the Frisch technique to the present investigation is that the retrieval of cloud droplet information is limited to drizzle free periods. This is a result of the radar sensitivity to large drops, and to the signal processing technique that was used to collect the data. The radar return is skewed to the large drops because in the Rayleigh scattering regime the radar reflectivity is proportional to the sixth power of the radius (Battan, 1973). In Frisch et al. (1995) (referred to herein as F95) the radar observations were processed using a pulse-pair algorithm that provides the mean radar reflectivity, reflectivity weighted Doppler velocity, and the spectrum width for a pulse volume. Pulse-pair estimates of the reflectivity and Doppler returns are dominated by the largest drops.

F95 was able to distinguish between drizzle-free periods by use of the pulse-pair Doppler radar spectrum width. Since the fall speed of a droplet is proportional to the drop diameter (e.g., Rogers, 1979), clouds containing cloud droplets and drizzle will have a larger spectrum width than those containing just cloud droplets. During periods of drizzle, F95 was able to characterize the drizzle microphysical characteristics using the three moments of the pulse pair algorithm.

Fox and Illingworth (1997) made aircraft measurements of clouds with FSSP and 2D cloud probes. Samples were collected in clouds containing an active drizzle process and in clouds that were drizzle free. They report that the presence of drizzle had little impact on the total liquid water content of the clouds. However, the presence of drizzle greatly impacted the magnitude of radar reflectivity and the vertical reflectivity profile. In drizzle free clouds, the radar reflectivity increased with height through the cloud, while the reflectivity factor in clouds with drizzle had less variation with height. Their measurements also indicate that the presence of drizzle had little effect on the effective radius of the cloud droplet population. The restriction of F95 to drizzle-free periods can be overcome if a correction to the radar reflectivity of drizzle can be applied.

One possible solution to the drizzle dilemma of F95 might be the addition of a lidar sensor, which is more sensitive to micron sized cloud droplets than radar. The retrieval of effective radius, for example, could be augmented with the lidar/radar backscatter ratio as described in Intrieri et al. (1993). Unfortunately, the Vandenberg area is well known for dense marine stratus (e.g., Noonkester, 1979; Vali et al., 1998). Visible optical depths in excess of 20 have been reported for coastal marine stratus off the coast of California by satellite based retrieval techniques (Szczodrak et al., 2001). The likelihood of encountering thick clouds at Vandenberg precludes the use of lidar in the present study.

Several investigators have demonstrated the utility of Doppler spectra for the retrieval of the drop-size distribution (e.g., Wakasugi et al, 1986; Babb et al., 1995; Gossard et al., 1997; Babb et al., 1999; Galloway et al., 1999) via a zenith pointing radar. The method is based on the laboratory measurements of Gunn and Kinzer (1949) that show that the fall speed of drops is proportional to the drop diameter. The Doppler spectrum of the fall rates, which is acquired through the use of a fast Fourier transform (FFT) signal processing algorithm, can be used to retrieve the droplet spectrum for the cloud and drizzle droplets. From this distribution the parameters needed to retrieve the optical depth can be obtained. The signal processing hardware of the radar used in the present study does not have the computational throughput necessary to fully implement this technique, but, as discussed in Section 5, can provide a first step towards correcting the contamination due to drizzle.

The present challenge is to measure the clouds with sensors that can penetrate through optically thick clouds while having adequate sensitivity to cloud droplets. The 35 GHz, Ka-band Air Force Cloud Profiling Radar (AFCPR) is an ideal tool for these measurements when used in the zenith pointing mode, given that the attenuation for dense fog is on the order of 1 dB/km (Skolnik,1990) and the radar sensitivity for a one-second integration is -40 dBZ at 2.5 km range.

2. RETRIEVAL PROCEDURE

The critical relationship utilized in F95 is that the radar reflectivity and MWR retrieved total integrated liquid are connected through moments of the drop size distribution. F95 used a lognormal distribution to approximate the cloud droplet spectrum. Frisch et al. (1998) cite that the technique is also applicable to other distributions such as the modified gamma.

The lognormal distribution is given by

$$\frac{dn(r)}{dr} = \frac{N}{r \ln \sigma \sqrt{2\pi}} e^{-\left[(\ln^2 r - \ln^2 r_o)/2\ln^2 \sigma\right]}, \quad (1)$$

where N is the droplet number density, σ is the distribution width, r is the radius, and r_o is the modal radius. The k^{th} moment of this distribution is given by

$$\left\langle r^k \right\rangle = r_o^k e^{(k^2\sigma^2/2)}. \quad (2)$$

Therefore, the 6^{th} moment of the distribution is related to the 3^{rd} moment by

$$\left\langle r_o^6 \right\rangle = \left\langle r_o^3 \right\rangle e^{9\sigma^2}. \quad (3)$$

The radar reflectivity factor, $Z = \sum_{vol} (2r_i)^6$ (e.g., Battan, 1973), at a particular height (h) in the cloud can be expressed in terms of the lognormal distribution by

$$Z(h) = 2^6 N(h)\left\langle r^6(h)\right\rangle = 2^6 N(h) r_o^6(h) e^{(18\sigma^2)}. \quad (4)$$

Likewise, the liquid water content (q), proportional to the 3^{rd} power of the radius, is given by

$$q(h) = \frac{4}{3}\pi\rho_w N(h) r^3(h) = \frac{4}{3}\pi\rho_w N(h)\left\langle r^3(h)\right\rangle = \frac{4}{3}\pi\rho_w N(h) r_o^3(h) e^{(9\sigma^2/2)}, \quad (5)$$

where ρ_w is the water density.

The total integrated water (Q) provided by the microwave radiometer is the sum of q through the depth of the cloud, where Δh is the radar range gate spacing.

$$Q = \sum_{i=1}^{M} q_i \Delta h \quad (6)$$

The effective radius (r_e) and modal radius (r_o) are related by

$$r_o = r_e e^{-2.5\sigma^2}. \quad (7)$$

Combining Eqs. (4), (5), and (6) with the substitutions from Eqs. (3) and (7), and solving for r_e

$$r_e(h) = \frac{Z^{1/6}(h)}{2Q^{1/3}}\left(\frac{\pi\rho_w}{6}\right)\left(\sum_{i=1}^{m} Z^{1/2}(h_i)\Delta h\right)^{1/3} e^{-2\sigma^2} \tag{8}$$

(Frisch et al., 2002).

Therefore, the effective radius can be determined directly from radar backscatter and MWR derived estimate of total liquid water.

It is assumed in Eq. (8) that the logarithmic width (σ) of the distribution is known and is the same at every level of the cloud. F95 assumed a width of σ=0.35. Miles et al. (2000) compiled drop size information of low level stratus clouds associated with a variety of measurement campaigns, including several in California. They report logarithmic widths to generally vary within the range of 0.24 to 0.40, but with outliers as large as 0.72.

F95 and the follow-on related works (Frisch et al., 1998, 2000, and 2002) assumed that the number density (N) is constant with height in the cloud. This assumption appears to be reasonable based on aircraft measurements of clouds (e.g., Slingo et al., 1982; Nicholls, 1986; Miles et al., 2000). Frisch also assumed that the number density is known. For continental and marine stratus clouds Frisch et al. (1995, 2002) used N =200 cm^{-3} and N =100 cm^{-3}, respectively. Herein, the number density is determined as a function of the liquid water content and the reflectivity structure:

$$N = \frac{36Q^2 e^{(9\sigma^2)}}{\pi^2 \rho_w^2 \left(\sum_{i=1}^{m} Z^{1/2}(h_i)\Delta h\right)} \tag{9}$$

For any particular radius within the spectrum, the number density is given by $n(\ln(r)) = Ne^{-\left[(\ln(r)-\ln(r_n))^2/2\sigma_x^2\right]}$.

Optical depth (τ) is given by

$$\tau = \pi\int_0^{\infty}\left[\int_0^{\infty} Q_{ext}(r)n(r,z)r^2 dr\right]dz, \tag{10}$$

where Q_{ext} is the optical extinction. Using an assumed width for the droplet spectrum, with the estimates of effective radius and number density, and the cloud thickness measured by radar, the optical depth at NIR wavelengths can be derived using Mie scattering theory. Mie calculations were carried out using the Wiscombe (1979, 1980) MIEV0 scattering code.

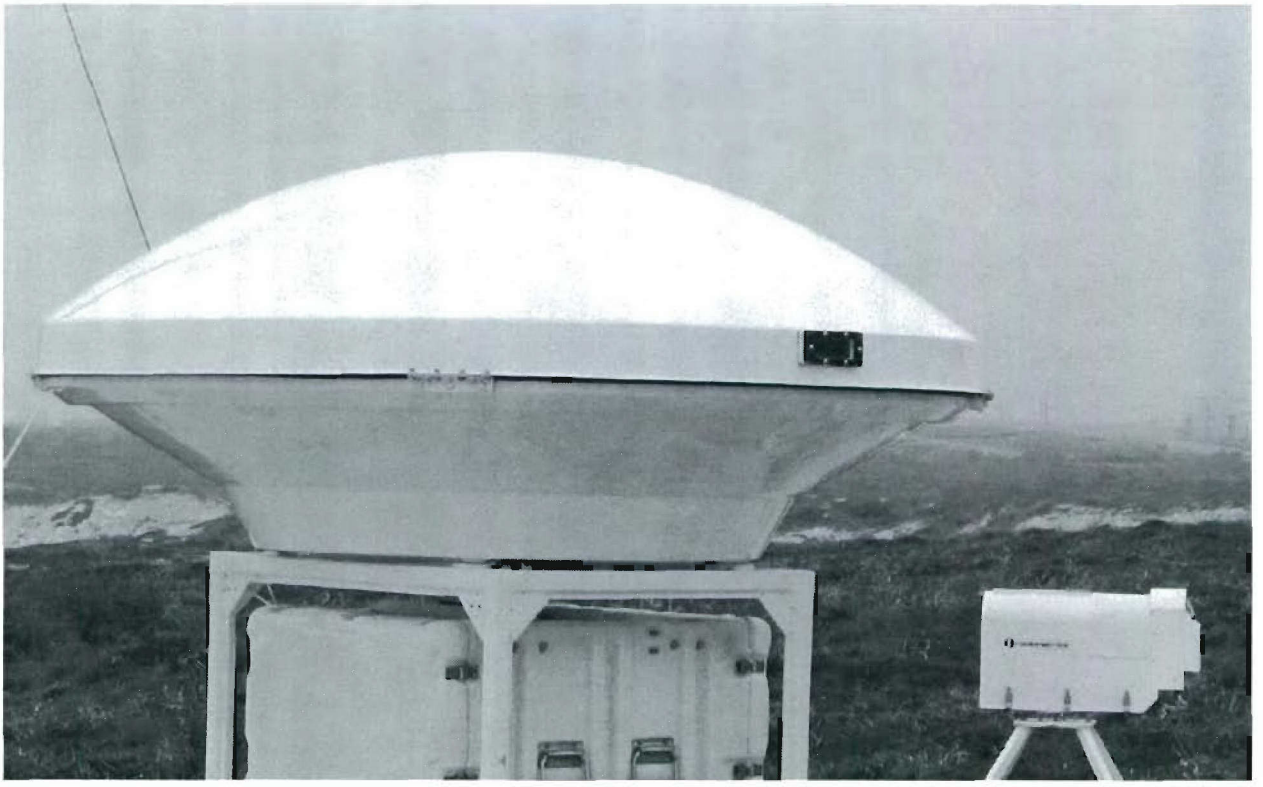

Figure 1. AFCPR radar and Radiometrics WVP-1500 microwave radiometer at the OS-45 Vandenberg AFB site.

3. SENSORS

Descriptions of the radar and radiometer sensors used in this study are provided below. Figure 1 shows the sensor setup at Vandenberg AFB.

3.1 Ka-band Radar

The Air Force Cloud Profiling Radar (AFCPR) is a mobile Ka-band Doppler radar that is well suited to cloud observations. The radar uses a 1.6 kW liquid-cooled Klystron transmitter that supports a 5% duty cycle. A 20,000 Hz Pulse Repetition Frequency (PRF) pulse rate is supported in the standard (pulse) mode where a 500 ns pulse width is used. In the pulse compression (chirp) mode a 12.8 μs pulse width is used. The pulse compression mode yields a 12 dB improvement in system sensitivity compared to the standard pulsed mode and is useful at ranges beyond 4 km. Range gate resolution is 75 m in both the pulse and the chirp mode.

The radar was calibrated just prior to shipment to Vandenberg using a 1.5" tetrahedral corner cube. The system calibration has been found to be very stable over time, varying by less than 1 dB over a 12 month period.

The radar has both pulse-pair and FFT signal processing algorithms. For the present investigation, the radar was operated in the FFT mode at a 4,000 Hz PRF yielding a ±8.6 Nyquist range. A 128 point FFT yielded 0.13 m/s Doppler resolution. The radar signal processing hardware could support a maximum of 64 range gates at this resolution. Given a range gate spacing of 75 m, data was collected to a range of 4.8 km. The radar was operated briefly in the regular pulse mode before and after each data collect to verify that there were no clouds at higher altitudes.

Specifics of the radar are provided in Table 1.

Table 1: AFCPR Specifications

Transmit frequency	35.03 GHz
Transmitter	1.6 kW Extended-Interaction Klystron Tube
Transmit modes	Pulse mode, linear-FM chirp, or interlaced
Duty cycle (maximum)	1% pulse; 5% chirp
PRF (maximum)	20,000 Hz (pulse); 3,906 Hz (chirp)
Nyquist velocity (maximum)	±42.8 m/s (pulse); ±8.2 m/s (chirp)
Range resolution	75 m
Receiver bandwidth	2 MHz
Noise figure	8 dB
Single-pulse sensitivity at 5 km range	-20 dBZ (pulse); -33 dBZ (chirp)
Antenna	1.8 m diameter cassegrain with radome
Antenna beamwidth, gain	0.30°, 53 dBi
Antenna sidelobes	-19.5 dB
Polarizations	Linear (HH and HV receive on alternate pulses)
Cross-Pol Isolation	-25 dB

3.2 Microwave Radiometer

The Radiometrics Inc. WVP-1500 Water Vapor Profiling Radiometer is a 5 channel microwave radiometer capable of accurate determination of the total integrated liquid water and the total integrated water vapor. The radiometer also provides the water vapor profile from 0 to 10 km AGL, at a resolution of 100 m up to 1 km altitude and 250 m at greater altitudes. Integrated sensors provide ground level measurement of temperature, relative humidity, and pressure. The radiometer was configured to save these parameters at a 5 minute interval for this study. Specifications for the WVP-1500 radiometer are provided in Table 2.

The radiometric quantities are determined in real-time through a neural network algorithm that was supplied with the radiometer. For optimal operation, the neural network algorithm is trained on a climatology of radiosondes for a particular region. Radiometrics Inc. provided the neural network training file for the Vandenberg AFB area.

Table 2: WVP-1500 Microwave Radiometer Specifications

Frequencies (GHz)	22.235, 23.035, 23.835, 26.235, 30.000
Accuracy	0.5 K
Resolution	0.25 K
Radiometric Range	0-700 K
Surface temperature accuracy	0.5 C
Surface humidity accuracy	2% relative humidity
Surface pressure accuracy	5%
Derived products	Total integrated liquid water, total integrated water vapor, water vapor profile from 0 to 10 km

The neural network retrieval method is shown to provide accurate retrievals over a wide variety of conditions (Ware, et al., 2004). For a comparison of the neural network performance relative to Newtonian iteration, regression, and Bayesian maximum probability techniques, see Solheim et al. (1996, 1998).

The radiometer brightness temperatures observations are calibrated through comparison with a calibrated noise diode and a reference black body temperature that is used to set the offset for the measurements. Radiometrics claims that this procedure minimizes measurement drift. Liljegren (1996) reports that the stability of the calibration of the Model 1100, an earlier Radiometrics design, was quite good, varying by less than 1% over a one month period.

In spite of the stability of the system, system calibrations are conducted on an hourly basis. This involves a tilting procedure to calibrate the noise diode. Several quality control procedures are applied automatically to ensure the validity of a calibration measurement, such as the absence of rain, as determined by the integrated rain sensor, and a homogeneous sky as determined by the tilting operation.

The radiometer is designed for all weather operation, although its accuracy is impacted when the sensor radome is covered by precipitation. An integrated blower system and a rain-sensor-activated heater eliminate moisture on the radome due to dew or drizzle.

4. EXPERIMENT DESCRIPTION

Two experiments were conducted at Vandenberg AFB in 2003: on 10 September in conjunction with a Minuteman III missile launch, and on 18 October in conjunction with the final Titan II launch. In both experiments the sensors were parked at the "OS-45" Vandenberg site that is used as an observation site by the media. OS-45 is located at 34.702° N and 120.582° W, which is about 8 km south of the Minuteman III launch site and about 5 km north of the Titan II launch site, and approximately 1 km east of the beach. A satellite picture of the area from http://terraserver.microsoft.com is provided in Figure 2.

Figure 2. Satellite view of the OS-45 Vandenberg AFB site where the radar and microwave radiometer sensors were located.

The Minuteman III launch was accompanied by fog that began during the evening of 9 September and lifted during the late morning of the 10th. Dense fog was observed at the radar site during the launch. Radar transmission began at 8:50 UTC (1:50 LST) and continued until 11:00 UTC (04:00 LST), at which time radar transmission was required to cease in preparation for the rocket launch. At 11:30 UTC the Minuteman III was launched. Radar transmission resumed at 11:40 UTC and continued until 18:17 UTC, by which time the fog had completely lifted and blue sky was observed overhead.

The Titan II launch occurred on the morning of 18 October at 16:17 UTC under clear skies. Because of the radio frequency sensitivity of the Titan II payload, the DMSP-53D military meteorological satellite, the radar was not allowed to transmit until 16:40 UTC. About 50 minutes of radar observations were collected. Radar silence resumed at 17:30 UTC. Because of

the cloud free conditions around the time of the launch, no useful radar or radiometer returns were observed.

The following discussion focuses on radar and microwave radiometer measurements associated with the Minuteman III launch.

5. DATA CONSIDERATIONS

The microwave radiometer was operated without incident for several days preceding and following the Minuteman III launch. It is not believed that the presence of drizzle impacted the quality of the radiometer data because the integrated blower system was successful in maintaining a dry radome.

The presence of fog complicates the analysis of the radar measurement. There are a several hardware issues that hinder the observation of near range targets. One consideration is the blind area caused by the receiver switching lag. For the AFCPR, the minimum detectible range caused by the switching lag is 15m. A second consideration for the detection of targets near the radar is contamination due to the receiver leakage within the first few range gates. The receiver leakage

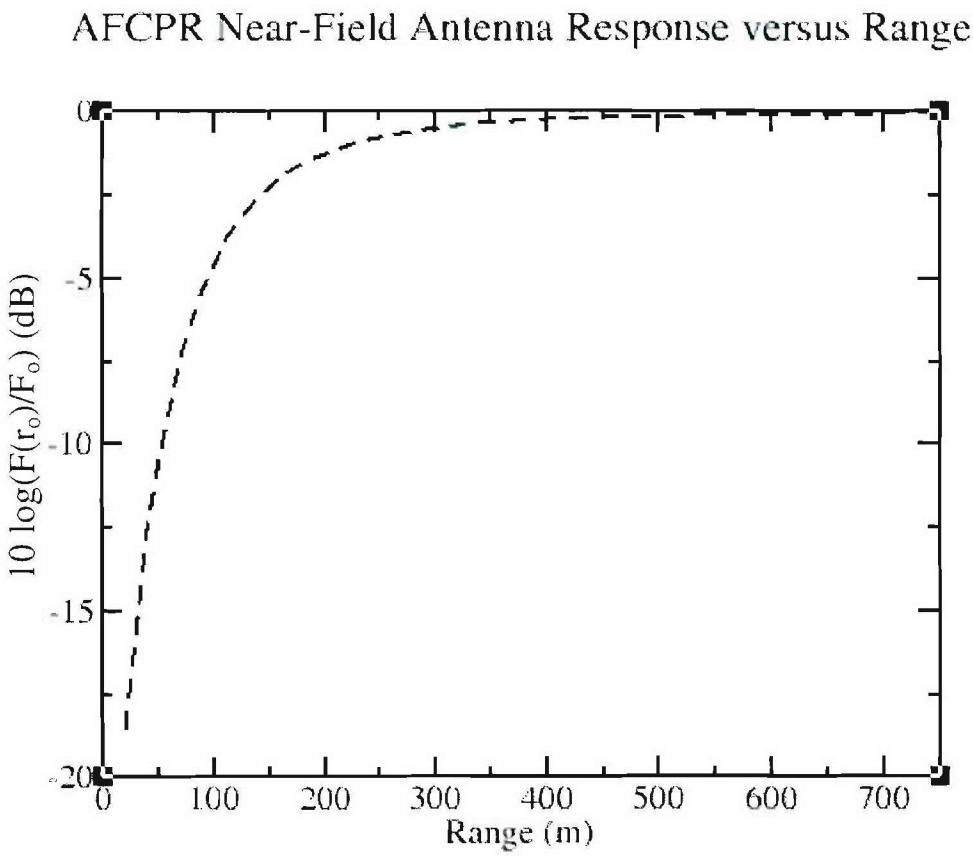

Figure 3. Theoretical antenna response curve for the AFCPR (Eq. (11)).

near the antenna is much stronger than the backscatter of a typical cloud. However, the backscatter is relatively steady and so can often be removed.

A third consideration is a reduction in antenna gain in the near field range where the antenna beam is not fully focused, resulting in a loss of system sensitivity. The AFCPR far field or Fraunhofer region, the range where the antenna gain is 99% of the gain at infinite range, is 750m. For the present study, where the fog extends into the radar near-field range, it is necessary to apply a correction to adjust for the antenna sensitivity. Sekelsky (2002) provides the following formulation for near-field antenna correction:

$$\frac{F(r_o)}{F_o} = \frac{5.26x10^{-5} + (r_o / r_f)^{2.5}}{0.011 + (r_o / r_f)^{2.5}}, \qquad (11)$$

where $F(r_o)/F_o$ is the near field reflectivity reduction, r_f is the far field range, and r_o is a near field range greater the 0.025 r_f. The calculated near-field antenna response for the AFCPR is given in Figure 3. In general the near-field adjustment is small but increases rapidly for ranges under 200m. Near-field adjustments were applied to the data. In these measurements the maximum adjustment applied was 3.8 dB at the first range gate which was centered at 112m,.

A fourth consideration for near range measurements is clutter. The primary source of clutter for a zenith pointing radar is dust and especially insects. Insects are useful tracers of the wind even for long wavelength systems like the WSR-88D (e.g., Miller et al., 1998). Ka-band radars, by virtue of a short wavelength, are very sensitive to insects, which have a backscatter comparable to water drops (Russell and Wilson, 1997). The large relative spacing of insects relative to the radar beam width, and the varied motion of insects relative to the wind results in a rather textured radar return that is the characteristic signature of insects. Insects tend to reside in the boundary layer up to the top of the mixed layer (Achtemeier, 1991). The 10 Sept. 2003, 12Z sounding at Vandenberg AFB (Figure 4) shows that the mixed layer to extended to about 1.5 km, the height of the primary clutter in the observations.

The radar observations were contaminated by receiver leakage and clutter during the entire observation period. It is necessary, therefore, to process the data in a manner that minimizes the impact of the contamination. Cloud discrimination is greatly aided by processing the radar observations with the FFT signal processing algorithm.

The spectrum of insect clutter is narrow and variable while the spectrum of a cloud is relatively wide and steady. This character of the cloud signature is due to an inherent distribution of droplet sizes and associated fall speeds. Figure 5 provides an excerpt from Gunn and Kinzer's (1949) laboratory measurements of droplet fall rate. Their measurements reveal the strong relationship between drop size and fall rate. The primary interest here is to characterize the cloud droplets, which are defined by a diameter of 0.2 mm or less (Huschke, 1959). According to the Gunn and Kinzer measurements, cloud droplets will have a maximum fall rate of 0.7 m/s in still air.

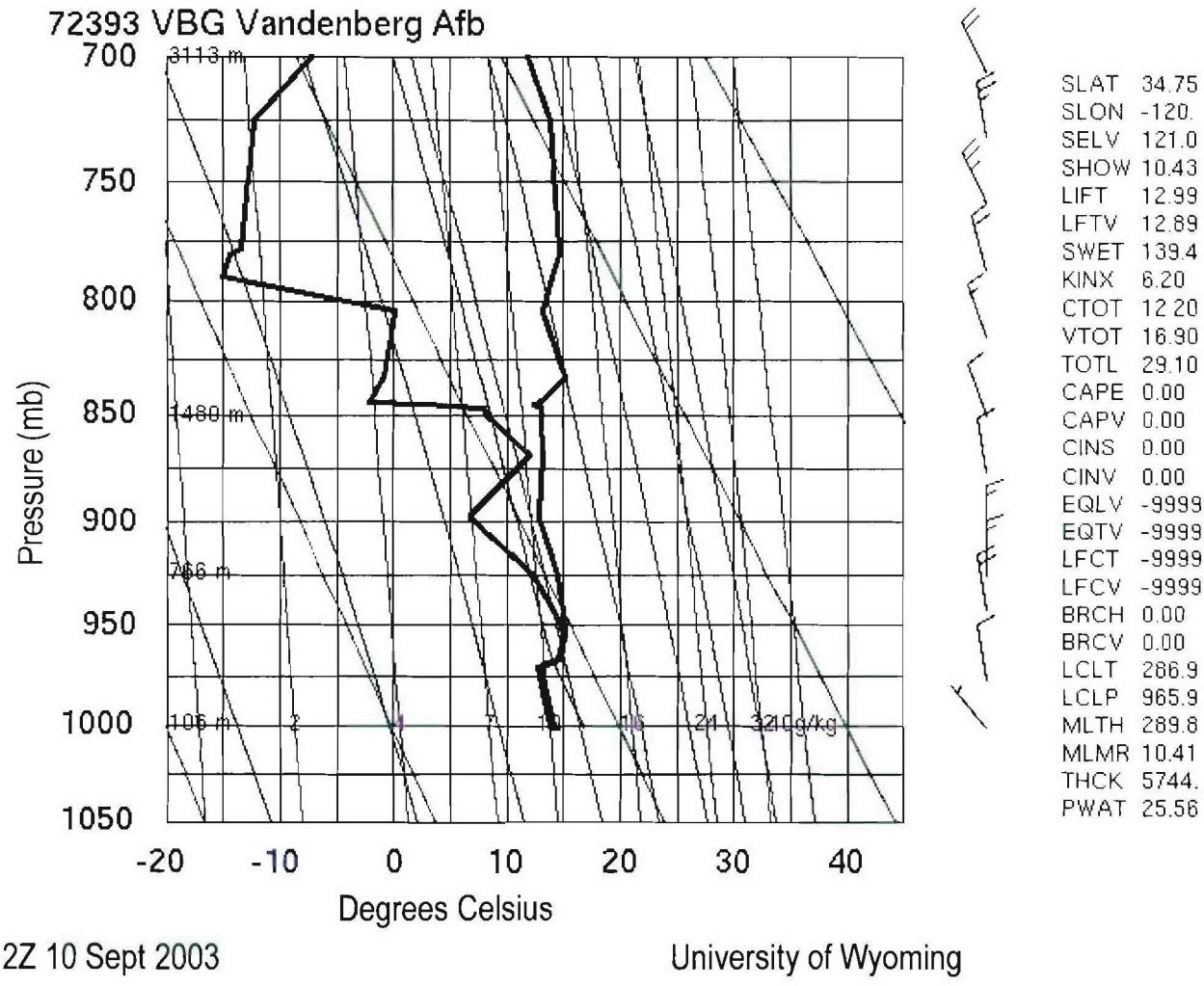

Figure 4. Vandenberg 12:00 UTC sounding.

In order to accurately describe the fog characteristics as seen in the radar observations it is necessary to remove the data contaminants and to correct for hardware limitations. A simple 4-element cloud detection algorithm and processing scheme was constructed to recover the cloud reflectivity information.

1) The first step in cleaning the data is to remove the receiver leakage contamination. A "clutter map" of the receiver leakage is generated during a cloud free period and is subtracted from the fog observations. Ideally, this process removes the leakage signal and allows for the recovery of the cloud information. In practice this approach yields mixed results because a small variation in transmitter output power can exceed the backscatter return of the cloud. The leakage subtraction process can result in an over- or underestimation of cloud backscatter in the first few range gates from the radar where the receiver leakage is strongest. Since the cloud spectrum is relatively wide, and the receiver leakage is centered at zero Doppler, the cloud reflectivity can be mostly recovered.

2) The Doppler spectrum from the FFT is also used to distinguish between clouds and insect clutter. It is assumed that clouds are comprised of a distribution of drop sizes and, therefore, a range of fall velocities. Whereas the spectrum associated with insects is narrow, the velocity spectrum of a cloud is rather broad. A fall rate of 0.4 m/s was found to be a reasonable cutoff for allowing detection of the cloud, while eliminating most of the artifacts.

3) An antenna response correction (Eq. (11)) is applied to the near field measurements.

4) The small gap in the radar data near the radar due to internal switching lag is filled in.

6. CASE STUDY AND RESULTS

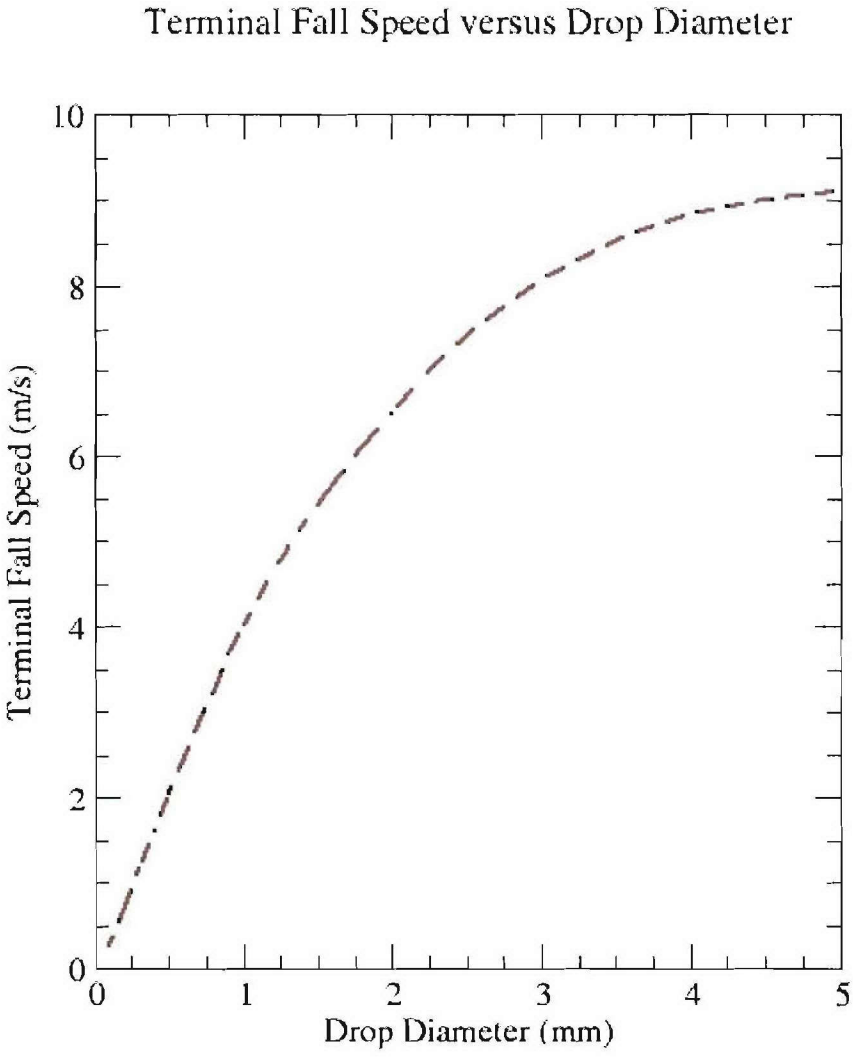

Figure 5. Terminal fall speed for liquid drops (from Gunn and Kinzer, 1949).

Figure 6 provides the microwave radiometer retrieved products and the weather sensor information during the period of measurement on 10 September 2003 when fog was observed. The retrieved water vapor profile at 11:29 UTC, just before the Minuteman III launch, is shown in the top panel of the figure. The primary moisture layer extends below 1 km AGL. The second panel from the top gives the integrated vapor over the observation period. A vertical

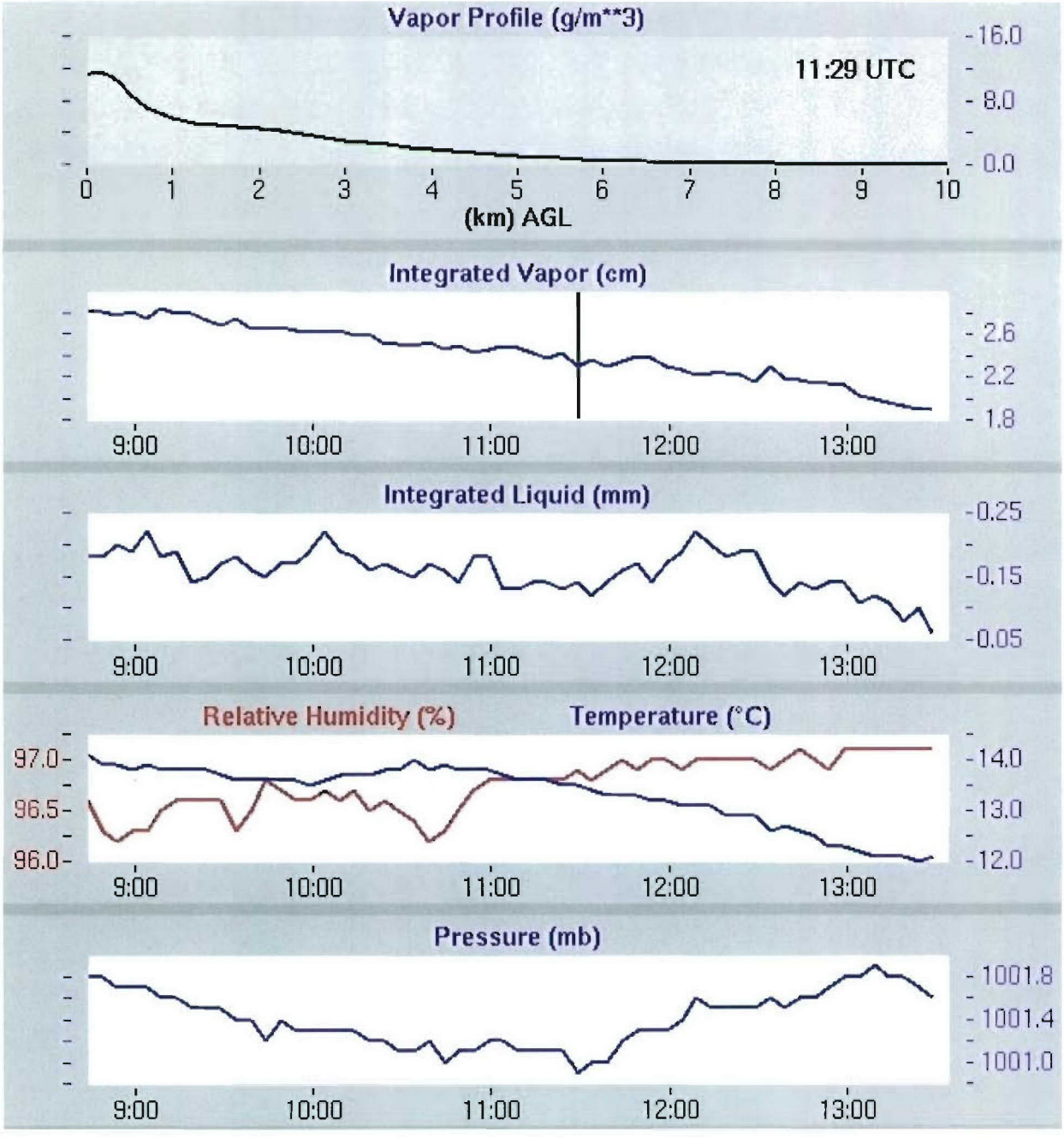

Figure 6. Microwave radiometer measured and retrieved parameters for the observation period on 10 September 2003.

black line in that panel identifies the 11:29 location. It is seen that there was a gradual decrease in the moist layer during the observation period.

In the third panel is shown the history of integrated liquid. Integrated liquid averaged 0.19 mm during the first 4 hours of the observation period and then declined until the first beaks in the clouds were visibly sighted at 13:30.

In the bottom two panels of Figure 6 the time histories of surface temperature, relative humidity, and pressure, obtained from the radiometer, are provided. These quantities varied little over the observation period.

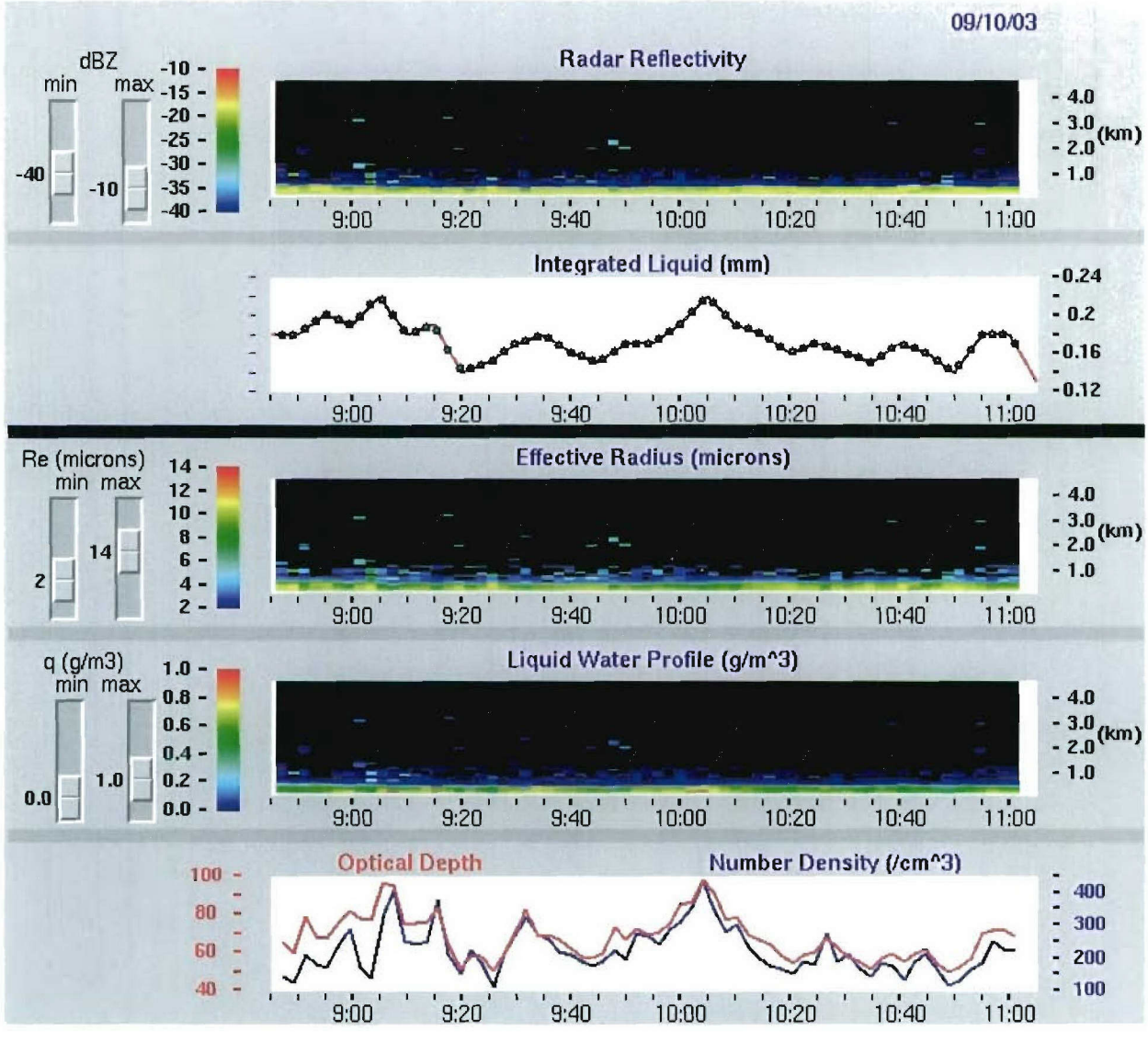

Figure 7. Radar and radiometer measurements (top panels) and retrieved parameters (bottom panels) before the 10 September 2003 Minuteman III launch.

Figures 7 and 8 provide the combined radar and microwave radiometer observations and retrievals before and after the rocket launch, respectively. The top panels show the radar reflectivity in standard dBZ (mm^6/m^3) units. Fog depth varied from 0.5 to 1.1 km during the observation period. The second panels provide the integrated liquid history. Overlaid circles correspond to the radar sample volume times.

Radar/radiometer retrieved values are provided in the lower 3 panels of the figures. The effective radius varied between 2.5 μm and 11.2 μm, and averaged 6.0 μm during the collection period. Liquid water, shown in the forth panel from the top, varied from 0.01 to 0.88 g/m^3, and averaged 0.26 g/m^3. Both effective radius and integrated liquid were found to decrease with height.

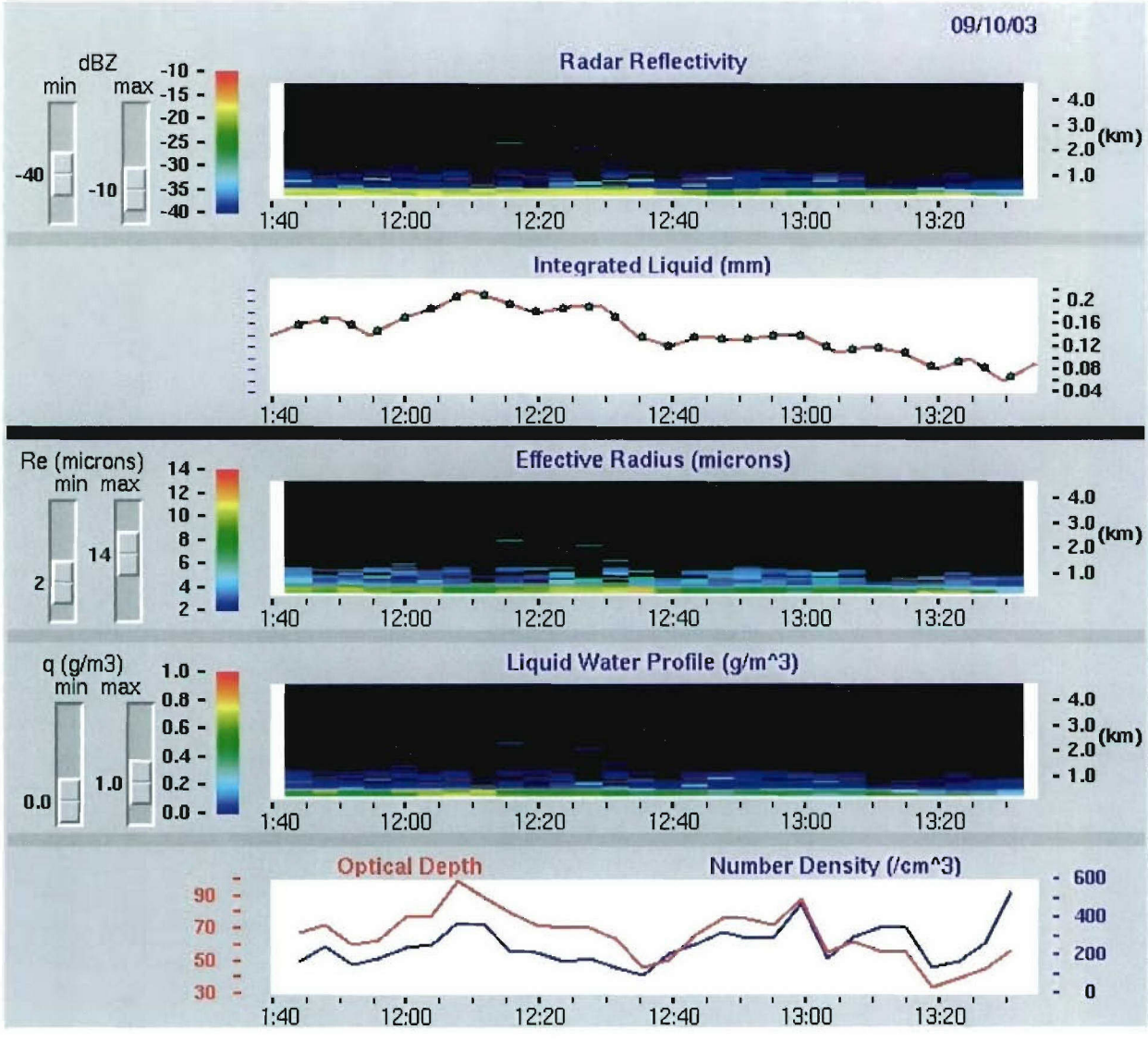

Figure 8. Radar and radiometer measurements (top panels) and retrieved parameters (bottom panels) after the 10 September 2003 Minuteman III launch.

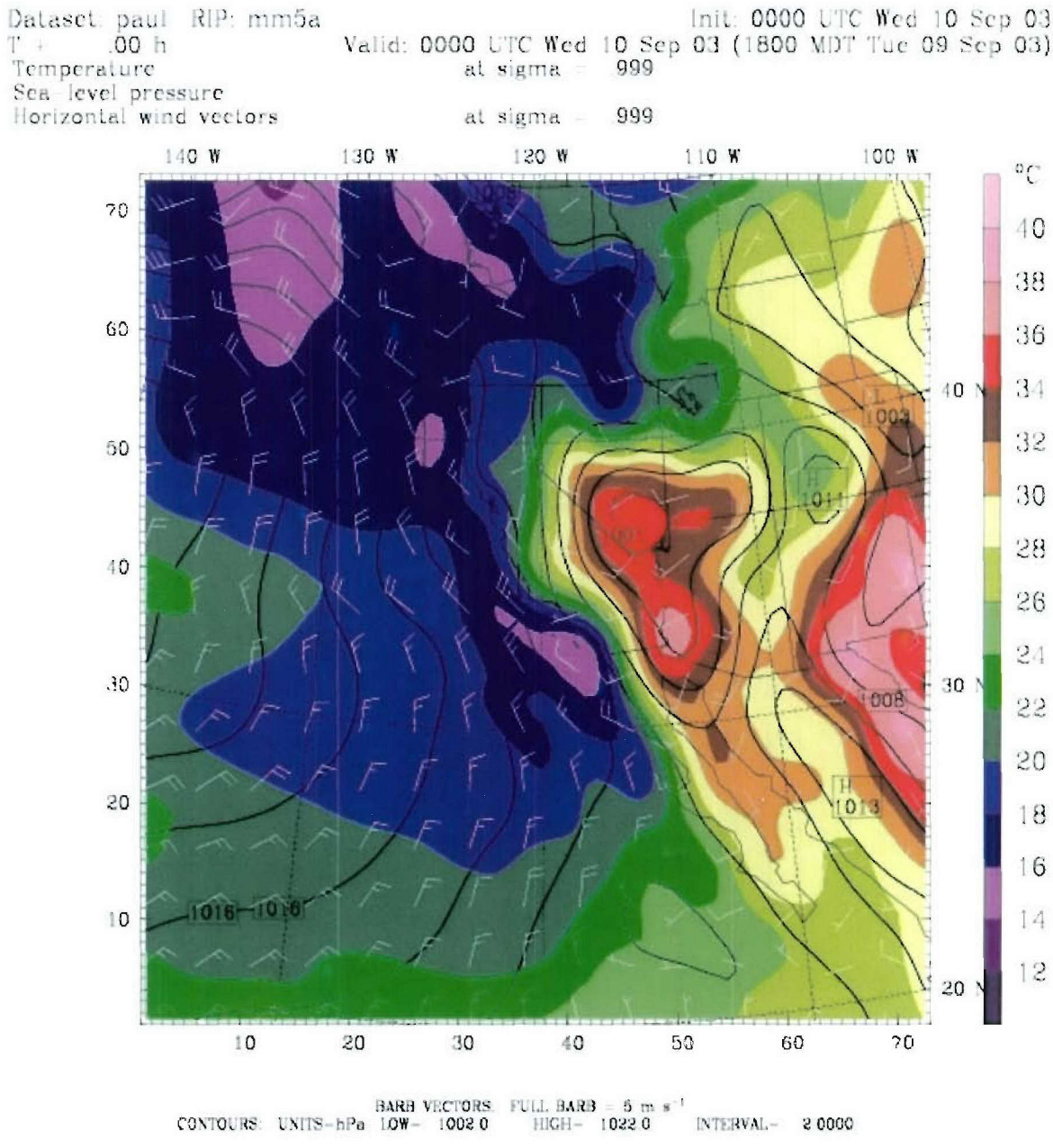

Figure 9. MM5 sea surface model initialization for 00:00 UTC 10 September 2003.

The bottom panels show the time histories of number density and optical depth. Number density varied from 107 cm^{-3} to 433 cm^{-3}, averaging 221 cm^{-3}, in the time period before the launch, and 94 cm^{-3} to 538 cm^{-3}, averaging 254 cm^{-3}, after the launch, which exceeds the value of 100 cm^{-3} used by Frisch (1995, 2002) for marine stratus clouds.

Feingold et al. (1999) show a wide variation in cloud number density populations retrieved from Doppler radar. Several measurement campaigns in the California region report number densities

for marine status that are considerably greater than those used in the Frisch studies. Noonkester (1984) made aircraft measurements of marine stratus off the coast of San Diego and reports densities as large as 296 cm^{-3} in the center of the cloud. Measurements of coastal fog and stratus collected from a television tower in San Francisco, Goodman (1977), show that number density can vary greatly depending on the trajectory relative to the coast. The lowest concentration, 89 cm^{-3}, was measured for a "maritime" event where the trajectory of cloud movement was directly from the west, over the ocean. Clouds associated with airflow trajectories that were initially from the west over water followed by a southern leg along several hundred kilometers of California coast were found to have increased number densities. In three of these so called "maritime-continental modified" trajectories the average number density was 143, 170, and 208 cm^{-3}. The largest number densities were found to be associated with clouds that followed a long coastal trajectory from the north. The largest of the average number densities in these "continental" trajectories was 317 cm^{-3}.

Figure 9 shows the Pennsylvania State University and National Center for Atmospheric Research mesoscale model (MM5) sea level initialization for 00:00 UTC on 10 September. The initialization shows a flow pattern consistent with the maritime-continental modified trajectories of Goodman (1977). Corroborating evidence is provided by the 12:00 UTC AFB sounding (Fig. 4) that indicates wind directions generally from the NNW. Under such flow conditions it is reasonable to assume that high cloud number densities prevailed. The retrieved number density prior to and after the launch was 222 cm^{-3} and 171 cm^{-3}, respectively.

Optical depth varied from 49.8 to 97.7, averaging 67.6, in the time period before the launch, and 34.0 and 99.3, averaging 65.5, after the launch. Just prior to and after the launch the optical depth was 67.9 and 67.2, respectively. Restricting the calculations to a number density of 100 cm^{-3}, as used by Frisch et al. (1995, 2002), the optical depth before and after the launch produced an optical depth estimate of 30.6 and 39.9, respectively (not shown).

Lastly, there appears to be a strong relationship between the optical depth and the integrated liquid. In fact, for this data set, the optical depth can be related simply to the integrated liquid (in units of mm) by the following relation:

$$\tau = 387 * Q. \qquad (12)$$

This relation yields an estimate of optical depth that differs by 18%, on average, from the radar and radiometer based retrieval, but only requires the use of the microwave radiometer.

References

Achtemeier, G. A. (1991): The Use of Insects as Tracers for "Clear Air" Boundary Layer Studies by Doppler Radar. *Journal of Atmospheric and Oceanic Technology*, **8**, 746-765.

Babb, D. M. and B.A. Albrecht (1995): Comparing 94-GHz radar cloud and precipitation drop spectra measurements with aircraft observations. Proc. 27th Int. Conf. on Radar Meteorology, Vail, CO, Amer. Meteor. Soc., 580-582.

Babb, D. M., J. Verlinde, and B. A. Albrecht (1999): Retrieval of cloud and precipitation drop distributions using 94 GHz radar Doppler power spectra. *J. Atmos. Oceanic Technol.*, **16**, 489-503.

Battan, L. J. (1973): *Radar Observation of the Atmosphere*. The University of Chicago Press, Chicago, 324 pp.

Cimini, D., E. Westwater, Y. Han, and S. Keihm (2003): Accuracy of Ground-Based Microwave Radiometer and Balloon-Borne Measurements During the WVIOP2000 Field Experiment, *IEEE Trans. Geosci. Rem. Sens.*, **41**, 2605-2615.

Feingold, G., A. S. Frisch, B. Stevens, and W. R. Cotton (1999): On the relationship among cloud turbulence, droplet formation and drizzle as viewed by Doppler radar, microwave radiometer, and lidar. *J. Geophys. Res.*, **104** (18), 22195-22203.

Fox, N.I. and A.J. Illingworth (1997): The retrieval of stratocumulus cloud properties by ground-based cloud radar. *J. Appl. Met.*, **36**, 485-492.

Frisch, A. S., C. W. Fairall and J. B. Snider (1995): On the measurement of stratus cloud and drizzle parameters with a Ka-band Doppler radar and a microwave radiometer. *J. Atmos. Sci.*, **52**, 2788-2799.

Frisch, A.S., G. Feingold, C.W. Fairall, T. Uttal and J.B. Snider (1998): On Cloud Radar and Microwave Radiometer Measurements of Stratus Cloud Liquid Water Profiles. *Journal of Geophysical Research*, **103**, 23195-23197.

Frisch, A. S., B. E. Martner, I. Djalalova, and M. R. Poellot (2000): Comparison of radar/radiometer retrievals of stratus cloud liquid water content profiles with in-situ measurements by aircraft. *J. Geophys. Res.*, **105**, 15361-15364.

Frisch, A. S., M. D. Schupe, I. Djalalova, G. Feingold, and M. Poellot (2002): The retrieval of stratus cloud droplet effective radius with cloud radars. *J. Atmos. and Oceanic Tech.*, **19**, 835-42.

Galloway, J., A. Pazmany, J. Mead, R. McIntosh, D. Leon, J. French, S. Haimov, R. Kelly, and G. Vali (1999): Coincident in situ and W-band radar measurements of drop size distribution in a marine stratus cloud and drizzle. *J. Atmos. Ocean Technol.*, **16**, 504-517.

Goodman, J. (1977): The microstructure of California coastal fog and stratus, *J. Appl. Meteor.*, **16**, 1056-1067.

Gossard, E. E., B. B. Snider, E. E. Clothiaux, B. Martner, J. S. Gibson, R. A. Kropfli, and A. S. Frisch (1997): The potential of 8 mm-radars for remotely sensing cloud drop size distribution. *J. Atmos. and Ocean. Tech.*, **14**, 76-87.

Gunn, R., and G. D. Kinzer (1949): The terminal velocity of fall for water drops in stagnant air. *J. Meteor.*, **6**, 243-248.

Hogg, D. C., F. O. Guiraud, J. B. Snider, M. T. Decker, and E. R. Westwater (1983): A steerable dual-channel microwave radiometer for measurement of water vapor and liquid in the troposphere, *J. Clim. Appl. Meteor.*, **22**, 789-806.

Huschke, R. E., Ed. (1959): *Glossary of Meteorology*. Amer. Meteor. Soc., 638 pp.

Intrieri, J. M., G. L. Stephens, W. L. Eberhard and T. Uttal (1993): A method for determining cirrus cloud particle sizes using a lidar and radar backscatter technique. *J. Appl. Met.*, **32**, 1074-1082.

Liljegren, J., and B. Lesht (1996): Measurement of Integrated Water Vapor and Cloud Liquid Water from Microwave Radiometers, International Geoscience and Remote Sensing Symposium (IGARSS), 21-26 May 1996, Lincoln NE.

Miles, N. L., J. Verlinde, and E.E. Clothiaux (2000): Cloud-droplet size distributions in low-level stratiform clouds, *J. Atmos. Sci.*, **57**, 295-311.

Miller, M. A., J. Verlinde, C. V. Gilbert, G. J. Lehenbauer, J. S. Tongue, and E. E. Clothiaux (1998): Detection of nonprecipitating clouds with the WSR-88D: A theoretical and experimental survey of capabilities and limitations. *Weather and Forecasting*, **13**, 1046-1062.

Nicholls, S., and J. Leighton (1986): An observational study of the structure of stratiform cloud sheets. Part I: Structure, *Quart. J. Roy. Meteor. Soc.*, **112,** 431–460.

Noonkester, V. R. (1979): Coastal marine fog in Southern California, *Mon. Wea. Rev.*, **107**, 830-851.

Noonkester, V. R. (1984): Droplet spectra observed in marine stratus cloud layers. *J. Atmos. Sci.*, **41,** 829–844.

Revercomb, H. E., Turner, D. D., Tobin, D. C., Knuteson, R. O., Feltz, W. F., Barnard, J., Bosenberg, J., Clough, S., Cook, D., Ferrare, R., Goldsmith, J., Gutman, S., Halthore, R., Lesht, B., Liljegren, J., Linne, H., Michalsky, J., Morris, V., Porch, W., Richardson, S., Schmid, B., Splitt, M., Vanhove, T., Westwater, E., and Whiteman, D. (2003): The Atmospheric Radiation Measurement (ARM) Program's water vapor intensive observation periods: overview, initial accomplishments, and future challenges, *Bull. Amer. Meteor. Soc.*, **84**, 217-236.

Rogers, R.R (1979): Initiation of Rain in Nonfreezing clouds, A Short Course in Cloud Physics, Chapter 7. Pergamon Press, 232 pp.

Russell, R.W. and J.W. Wilson (1997): Radar-observed "fine lines" in the optically clear boundary layer: Reflectivity contributions from aerial plankton and its predators. *Boundary Layer Meteorology*, **82,** 235-262.

Sekelsky, S. M (2002): Near-field reflectivity and antenna boresight gain corrections for millimeter-wave atmospheric radars, *J. Atmos. Oceanic Tech.*, **19**, 468-477.

Skolnik, M. I. (1990): *Radar Handbook*, Second Edition, McGraw Hill, Inc.

Slingo, A., R. Brown, and C. L. Wiench (1982): A field study of nocturnal stratocumulus; III. High resolution radiative and microphysical observations, *Quart. J. Roy. Meteor. Soc.*, **108,** 145–166

Solheim, F., J. R. Godwin, R. Ware (1996): *Microwave Radiometer for Passively and Remotely Measuring Atmospheric Temperature, Water Vapor, and Cloud Liquid Water Profiles*, Final Contract DAAL01-96-2009 Report, White Sands Missile Range.

Solheim, F., J. Godwin, E. Westwater, Y. Han, S. Keihm, K. Marsh, and R. Ware (1998): Radiometric Profiling of Temperature, Water Vapor, and Cloud Liquid Water using Various Inversion Methods, *Radio Science*, **33**, 393-404.

Solheim, F., J. Godwin, and R. Ware (1998): Passive ground-based remote sensing of atmospheric temperature, water vapor, and cloud liquid water profiles by a frequency synthesized microwave radiometer, *Meteorologische Zeitschrift*, **7**, 370-376.

Stephens, G.L. (1978): Radiation profiles in extended water clouds. II: Parameterization schemes. *J. Atmos. Sci.*, **35**, 2123-2132.

Szczodrak, P. H. Austin and P. B. Krummel (2001): Variability of optical depth and effective radius in marine stratocumulus clouds, *J. Atmos. Sci.*, **58**, 2912-2926.

Vali, G., R. D. Kelly, J. French, S. Haimov, D. Leon, A. Pazmany, and R. E. McIntosh (1998): Finescale structure and microphysics of coastal stratus. *J. Atmos. Sci.*, **55**, 3540-3564.

Wakasugi, K., A. Mizutani, M. Matsuo, S. Fukao and S. Kato (1986): A direct method for deriving drop-size distributions and vertical air motions from VHF Doppler radar spectra. *J.*

Atmos. Oceanic Technol., **3**, 623-629.

Ware, R., P. Herzegh, F. Vandenberghe, J. Vivekanandan, and E. Westwater (2004) (in review): Ground-Based Radiometric Profiling during Dynamic Weather Conditions, *J. Appl. Meteor.*

Westwater, E., Y. Han, and F. Solheim (2000): Resolution and accuracy of a multi-frequency scanning radiometer for temperature profiling, *Microwave Radiometry and Remote Sensing of Earth's Surface and Atmosphere*, Pampaloni and Paloscia (editors), VSP (publisher), The Netherlands, 129-135.

Wiscombe, W. J. (1979): *Mie Scattering Calculations: Advances in Technique and Fast Vector Speed Computer Codes*, Document PB301388, NTIS, Springfield, VA 22161.

Wiscombe, W. J. (1980). Improved Mie scattering algorithms. *Appl. Opt.*, **19**, 1505-1509.